ELSEVIER

Thermochimica Acta 397 (2003) 49–53

thermochimica acta

www.elsevier.com/locate/tca

Subsolidus binary phase diagram of $C_{10}Zn/C_{12}Zn$

Kezhong Wu, Ping Zuo, Xiaodi Liu*, Yajuan Li

Department of Chemistry, Hebei Normal University, Shijiazhuang, Hebei 050016, PR China

Received 3 November 2001; received in revised form 25 April 2002; accepted 29 April 2002

Abstract

Decylammonium tetrachlorozincate (n-$C_{10}H_{21}NH_3)_2ZnCl_4$ ($C_{10}Zn$) and dodecylammonium tetrachlorozincate (n-$C_{12}H_{25}NH_3)_2ZnCl_4$ ($C_{12}Zn$) were synthesized and a series of their mixtures $C_{10}Zn/C_{12}Zn$ were prepared. The experimental binary phase diagram of $C_{10}Zn/C_{12}Zn$ was established by means of differential scanning calorimetry (DSC) and X-ray diffraction. In the phase diagram a stable solid compound (n-$C_{10}H_{21}NH_3$)(n-$C_{12}H_{25}NH_3$)$ZnCl_4$($C_{10}C_{12}Zn$) and two eutectoid invariants were observed. It is noticeable that the phase diagram contains solid solution ranges.

Keywords: Decylammonium tetrachlorozincate; Dodecylammonium tetrachlorozincate; DSC; X-ray; Phase diagram

1. Introduction

The alkylammonium tetrachlorometallates(II) (C_nM) are organometallic compounds with the general formula (n-$C_nH_{2n+1}NH_3)_2MCl_4$. Their crystal structure results from the piling of sandwiches in which the inorganic layer MCl_4^{2-} is sandwiched between two alkylammonium layers, similar to perovskites. As potential solid–solid phase change materials (PCMs) C_nM has some advantages such as small change in volume, no volatilization, high enthalpies and low phase transition temperatures. The capability of C_nM for energy storage and their structure have been previously researched [1–5]. Busico et al. [6] studied binary C_nZn systems. The binary phase diagram for C_nM is reported elsewhere [7], but the phase diagram for $C_{10}Zn/C_{12}Zn$ is not known. In this paper $C_{10}Zn$ and $C_{12}Zn$ are synthesized and the subsolidus binary phase diagram of $C_{10}Zn/C_{12}Zn$ is obtained by DSC and X-ray diffraction. The phase diagram of $C_{10}Zn/C_{12}Zn$ is different from that of similar systems in the literature.

2. Experimental

2.1. Sample preparation

$ZnCl_2$, concentrated HCl and absolute ethanol used were analytical grade. Decylamine (CP) was purchased from Beijing Xudong Chemical Plant, dodecylamine (CP) from Tianjin Xiqing Kelong Reagent Plant.

$C_{10}Zn$ and $C_{12}Zn$ were prepared [7] and analyzed with an MT-3 CHN elemental analyzer (Japan). The results of elemental analysis are in wt.%, $C_{10}Zn$: C% 45.68 (45.86); H% 9.27 (9.24); N% 5.27 (5.35); $C_{12}Zn$; C% 50.09 (49.71); H% 9.54 (9.73); N% 4.88 (4.83) (note: experimental value (calculated value)). The products, $C_{10}Zn$ and $C_{12}Zn$, were weighed exactly in desired proportion to prepare different mixed samples. The two components were dissolved in absolute ethanol, then part of the solvent was evaporated.

* Corresponding author.

0040-6031/02/$ – see front matter
PII: S0040-6031(02)00316-7

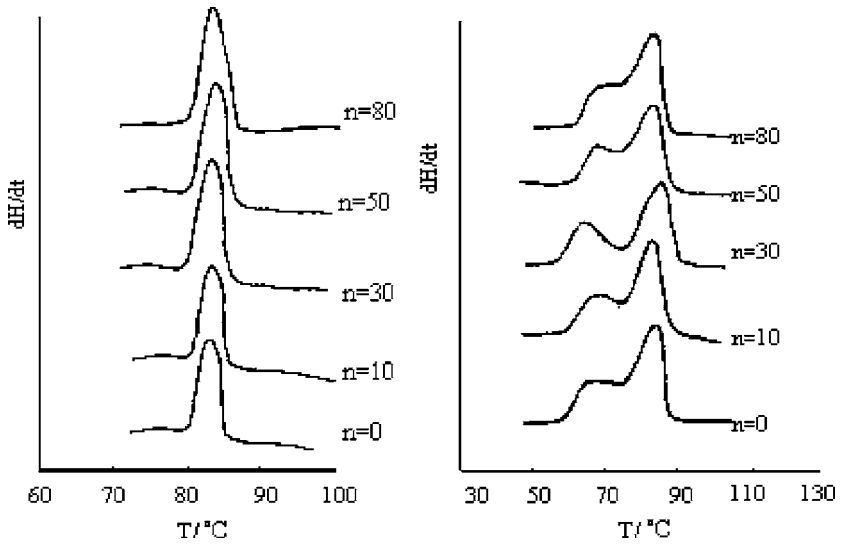

Fig. 1. The DSC curves of $C_{10}Zn$ and 22.72% $C_{10}Zn/C_{12}Zn$ after *n* heating–cooling cycles.

Air-dry samples were put into a vacuum desiccator for 8 h at about 80 °C.

2.2. DSC

The thermal behavior of the samples was investigated with a CDR-1 differential scanning calorimeter (DSC; Shanghai Scale Instrument Plant) at a scanning rate of 5 °C/min in a static atmosphere. Samples weighing about 5 mg were sealed in aluminum, crucibles. Transition enthalpies were obtained with KNO_3 as a reference standard ($\Delta H = 53.76$ J/g). The transition temperatures of $C_{10}Zn$ and $C_{12}Zn$ are identical with those of literature [5].

The samples including $C_{10}Zn$, $C_{12}Zn$ and their mixtures were investigated by DSC after several heating–cooling cycles around the transition temperature. The DSC curves and transition temperatures of thermally treated products were invariant. Fig. 1 shows the DSC curves of $C_{10}Zn$ and 22.72% $C_{10}Zn/C_{12}Zn$ after *n* heating–cooling cycles.

2.3. X-ray diffraction

X-ray diffraction patterns on compacted samples of the powders were taken by D/MAX-RA X-ray diffractometer (made in Japan) using Cu Kα radiation.

3. Experimental results

3.1. Thermal analysis

The results of DSC experiments obtained with "shape factors method" [8] are listed in Table 1. The data show that with increasing $\chi_{C_{10}Zn}$, the transition temperature of the system decreases. The first eutectoid temperature (about 57 °C) appears in the range of 19.08–35.00%. Then the transition temperature first rises, then drops. The second eutectoid temperature at about 52 °C was found from 55.10 to 76.32%. With $\chi_{C_{10}Zn}$ increasing gradually, the phase change temperature rises again. The table reveals that the first eutectoid temperature was not observed close to $\chi_{C_{10}Zn} = 0\%$, nor does the second end near $\chi_{C_{10}Zn} = 100\%$. The range of the first eutectoid temperature does not end close to the beginning of the second. These observations indicate miscibility regions at the left and right boundary and middle of the phase diagram.

Calorimetry of the samples from 19.08 to 76.32% was carried out. The data are reported in Table 2. A ΔH–X chart (Fig. 2) was drawn to determine the composition of eutectoid point (x_e) and the boundaries of eutectoid invariant. When x deviates from the composition of the eutectoid point (increase or decrease), the peak (DSC) of the eutectoid weakens

Table 1
Solid–solid transition temperature of $C_{10}Zn/C_{12}Zn$ system

$\chi_{C_{10}Zn}$ (%)	T_{e_2} (°C)	T_{e_1} (°C)	T_o (°C)	T_f (°C)
0 ($C_{12}Zn$)			88	
0.81			87	88
4.11			84	87
8.70			79	85
10.08			78	84
13.09			76	83
16.50			72	81
19.08		57		80
22.72		58		76
30.09		57		74
35.00		57		76
41.14			63	77
47.82			70	78
51.37			61	75
55.10	52			70
58.71	52			66
62.68	53			61
67.99	52			59
71.28	52			61
76.32	51			68
83.17			57	74
88.86			70	77
93.06			75	79
99.16			80	81
100 ($C_{10}Zn$)			81	

Note: T_e, eutectoid invariant; T_o, onset temperature; T_f, finish temperature.

gradually, and the peak of excessive component becomes stronger and stronger. Therefore, according to the characteristic that the enthalpies of the eutectoid (ΔH_e) have a maximum and the enthalpies of excessive component (ΔH) have a minimum at the composition of the eutectoid point, we have drawn a ΔH–X chart to determine x_e [9]. Besides when $\Delta H_e = 0$, the eutectoid disappears at the boundary of eutectoid invariant. From Fig. 2, we find $x_e = 24.0$ and 63.2%. The first eutectoid invariants ranges from 18.5 to 41.0%, the second from 53.5 to 80.0%.

Table 2
ΔH-data for $C_{10}Zn/C_{12}Zn$ system

$\chi_{C_{10}Zn}$ (%)	ΔH_e (J/g)	ΔH (J/g)
19.08	24.32	70.93
22.72	85.86	24.50
30.09	62.90	25.14
35.00	35.64	41.05
55.10	14.56	65.00
58.71	42.15	42.15
62.68	62.27	11.10
67.99	51.68	31.41
71.28	35.46	43.55
76.32	19.08	72.50

3.2. X-ray diffraction

X-ray diffraction patterns are convenient for phase analysis, because the interplanar spacing d and relative intensity I are intrinsic properties of substances. Table 3 summarizes the d values of strong peaks with bigger relative intensity at room temperature for pure $C_{10}Zn$, $C_{12}Zn$ and their mixtures. We find d values of samples from 0.81 to 13.09% are similar to those of pure $C_{12}Zn$. This shows they are in a single-phase region. That is to say, in this concentration range, $C_{10}C_{12}Zn$ dissolves in $C_{12}Zn$ to form a solid solution (α). Similarly, samples from 83.17 to 99.16% and pure $C_{10}Zn$ have homologous patterns showing that $C_{10}C_{12}Zn$ dissolves in $C_{10}Zn$ to form a solid solution (β). In the same way, samples of 41.14, 47.82 and 51.37% are in a single-phase (γ) which is $C_{10}Zn$ or $C_{12}Zn$ dissolved in $C_{10}C_{12}Zn$. Samples from 16.50 to 35.00% are in the two-phase region, and their patterns are the overlap of α and γ. Similarly, the patterns from 55.10 to 76.32% are the overlap of β and γ, they are in the two-phase region. These facts indicate that the $C_{10}Zn/C_{12}Zn$ phase diagram has partial miscibility regions.

3.3. Establishment of phase diagram

The binary phase diagram of $C_{10}Zn/C_{12}Zn$ (Fig. 3) was obtained. According to the T–X and ΔH–X relations from the DSC and X-ray diffraction experiments.

4. Discussion

Fig. 3 indicates an intermediate $(C_{10}H_{21}NH_3)$-$(C_{12}H_{25}NH_3)ZnCl_4$ [10] is formed. At room temperature, the pure salts and their mixtures are ordered. Alkylammonium chains are parallel to each other and slightly tilted with respect to the normal of the inorganic layers. The chains are hydrogen bonded to $ZnCl_4^{2-}$. When the temperature goes up to 52 °C, the first eutectoid invariant occurs from 55.10 to 76.32%. $C_{10}Zn$ and $C_{10}C_{12}Zn$ undergo a reversible solid–solid

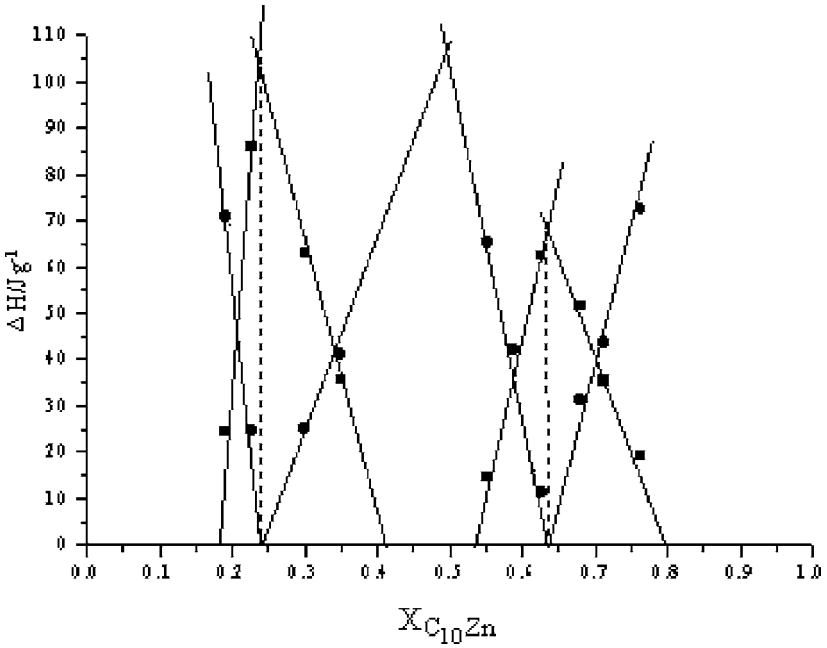

Fig. 2. ΔH–X relations for $C_{10}Zn/C_{12}Zn$ system.

Table 3
d-values at room temperature

$\chi_{C_{10}Zn}$ (%)	*d*												
0 ($C_{12}Zn$)	7.093	5.838	5.340	5.113	4.720		4.169	3.932	3.670	3.549		3.038	2.657
0.81	7.093	5.841	5.336	5.115	4.723	4.242	4.169	3.934	3.672	3.547		3.038	2.658
4.11	7.093	5.841	5.336	5.109	4.718		4.169	3.932	3.671	3.547		3.037	2.657
8.70	7.085	5.849	5.329	5.127	4.716		4.172	3.925	3.671	3.549		3.039	2.657
10.08	7.117	5.852	5.349	5.123	4.723		4.178	3.934	3.678	3.557		3.044	2.661
13.09	7.089	5.833	5.338	5.115	4.718	4.238	4.168	3.929	3.669	3.544		3.035	2.655
16.50	7.089	5.849	5.338	5.115	4.718		4.172	3.927	3.672	3.546	3.417	3.034	2.656
19.08	7.073	5.982	5.338	5.103	4.711		4.169	3.921	3.668	3.547	3.345	3.036	2.657
22.72	7.097	6.002	5.358	4.989	4.725		4.182	3.939	3.681	3.558	3.424	3.041	2.659
30.09	7.058	5.873	5.336	4.975	4.716		4.169	3.920	3.671	3.537	3.415	3.031	2.653
35.00	7.050	5.950	5.311	4.969	4.697		4.165	3.921	3.665	3.536	3.413	3.030	2.650
41.14		5.604	5.326	4.975	4.713		4.178		3.677	3.551	3.422		
47.82		5.615	5.333	4.993	4.720		4.180		3.679	3.553	3.422		
51.37		5.590	5.321	4.971	4.710		4.171		3.672	3.548	3.415		
55.10	6.005	5.625	5.330	4.993	4.578		4.178		3.677		3.424	3.107	2.672
58.71	6.008	5.620	5.295	4.987	4.574		4.173		3.677		3.418	3.106	2.673
62.68	5.940	5.554	5.251	4.938	4.487		4.141		3.650		3.397	3.091	2.657
67.99	5.996	5.610	5.289	4.983	4.536		4.176		3.677		3.422	3.110	2.673
71.28	6.019	5.622	5.300	5.000	4.563		4.196		3.690		3.430	3.116	2.677
76.32	6.008	5.597	5.271	4.987	4.534		4.172		3.674		3.419	3.108	2.676
83.17	6.199	5.525	5.198		4.486		4.138	3.733	3.649		3.398	3.104	2.665
88.86	6.242	5.564	5.208		4.513		4.160	3.752	3.666		3.411	3.122	2.676
93.06	6.275	5.587	5.381		4.531		4.179	3.762	3.681		3.423	3.130	2.684
99.16	6.278	5.597	5.238		4.528	4.261	4.172	3.766	3.680		3.422	3.129	2.683
100 ($C_{10}Zn$)	6.227	5.549	5.206		4.502	4.262	4.150	3.741	3.660		3.403	3.116	2.672

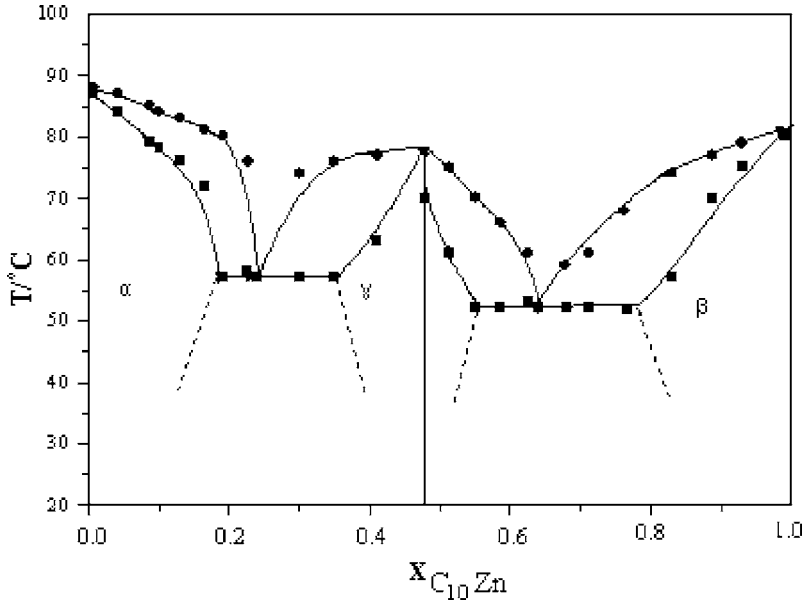

Fig. 3. Phase diagram of $C_{10}Zn/C_{12}Zn$ system.

phase transformation. In this situation, the chains are in a large degree of motional freedom and a disordered phase appears. At the same time, the hydrogen bonds are weakened and even destroyed. When the temperature increases to 57 °C, the second eutectoid invariant appears from 13.09 to 35.00%. Similarly, $C_{12}Zn$ and $C_{10}C_{12}Zn$ undergo ordered–disordered transition.

A binary phase diagram for a homologous system was reported [7], the shape of which is similar to ours. The largest difference is that their diagram shows absolute immiscibility, ours, partial miscibility. Binary system phase diagrams are determined by the difference of the two components. If their structure and size are little different, they often dissolve in each other and form miscible systems. Conversely, when they are much different, the degree of miscibility is limited. $C_{10}C_{12}Zn$ can be seen as $C_{10}Zn$ and $C_{12}Zn$ with one chain of each exchanged, so their structure and molecular size have little difference, which results in their partial miscibility.

References

[1] M.R. Ciajolo, P. Corradini, V. Pavone, Acta Cryst. B33 (1977) 553–555.
[2] C. Carfagna, M. Vacatello, P. Corradini, Gazz. Chim. Ital. (1977) 107.
[3] D.S. Zhang, D.S. Ruan, T.P. Zhang, Q.Z. Hu, D.Q. Xing, New Energy Sources 16 (1994) 39–42 (in Chinese).
[4] J. Fenrych, E.C. Reynhardt, S. Jurga, K. Jurga, Mol. Phys. 78 (1993) 1117–1128.
[5] D.S. Ruan, T.P. Zhang, D.S. Zhang, S.Y. Liang, Q.Z. Hu, Acta Energiae Solaris Sinica 16 (1994) 19–24 (in Chinese).
[6] V. Busico, T. Tartaglione, M. Vacatello, Thermochim. Acta 62 (1983) 77–86.
[7] W.P. Li, D.S. Zhang, T.P. Zhang, T.Z. Wang, D.S. Ruan, Thermochim. Acta 326 (1999) 183–186.
[8] R. Courchinoux, N.B. Chanh, Y. Haget, Thermochim. Acta 128 (1988) 45–53.
[9] U. Wiesner, W. Bieger, G. Krabbes, Thermochim. Acta 290 (1996) 115–121.
[10] V. Salerno, A. Grieco, M. Vacatello, J. Phys. Chem. 80 (1976) 2444–2448.